

**Electron-spin resonance of Gd in LaNi₅ single crystals:
Resolved fine structure in hexagonal host and the role of random strains**

R. Levin, A. Grayevsky, D. Shaltiel, V. Zevin, and D. Davidov
Racah Institute of Physics, The Hebrew University of Jerusalem, Jerusalem, Israel
(Received 7 February 1979)

Electron-spin resonance (ESR) of Gd in LaNi₅ single crystals exhibits partially resolved ESR spectra in the helium temperature range appropriate to Gd in hexagonal environment. This is interpreted by the small Korringa broadening with respect to the hexagonal crystalline-field parameter D , as well as by the absence of bottleneck in the relaxation mechanism. A line-shape analysis together with axial spin Hamiltonian yields $D = 250 \pm 30$ G and an isotropic g value: $g = 1.85 \pm 0.01$. The ESR spectra is shown to be affected significantly by the presence of random stresses. The Barnes-Plefka theory together with a random stress model can explain all the experimental features satisfactorily. It is pointed out that random stresses are a common feature to many single crystals of dilute alloys. In particular, the ESR spectra of LaSb:Gd published previously is reanalyzed in terms of our stress model. Annealing of our LaNi₅:Gd single crystals leads to the appearance of a "ferromagnetic resonance" appropriate to hexagonal symmetry. The origin of this resonance is probably associated with induced magnetic domains by slight chemical changes in the strongly exchange enhanced LaNi₅ host.

I. INTRODUCTION

Electron-spin resonance of Gd in hexagonal metallic single crystals like Mg:Gd,¹ Y:Gd,² Lu:Gd,³ and Sc:Gd,^{3,4} have been reported previously. In all these systems a single line was observed (rather than seven lines) with a large axial anisotropy in both the field for resonance and the linewidth at low temperatures. The field for resonance strongly depends on frequency and temperature. These general features were interpreted by an axial spin Hamiltonian as well as by the existence of bottleneck in the relaxation mechanism.^{2,3,5} The bottleneck effect creates a phase coherence between the spins of the Gd ions and those of the conduction electrons leading to a fine-structure narrowing.⁵⁻⁸ To the best of our knowledge, no report exists at present about resolved fine structure of Gd in hexagonal systems.

The present paper reports ESR study of Gd in annealed and as casted (unannealed) samples of LaNi₅ single crystals. The intermetallic compound LaNi₅ is an exchange-enhanced hexagonal paramagnet with relatively high density of states at the Fermi level.⁹ It has attracted considerable attention recently due to its excellent hydrogen absorption and desorption properties.^{10,11} Therefore, a study of the electronic, magnetic, and metallurgical properties of the LaNi₅ host, using Gd ESR as a probe, is most desirable. Previous ESR studies of LaNi₅:Gd powdered samples¹²⁻¹⁴ have shown a large negative Gd g shift which is concentration independent for low-Gd concentrations. This indicates the absence of bottleneck effect in the

relaxation mechanism.

Our experimental results on unannealed LaNi₅:Gd single crystals have shown partially resolved spectra (three lines) for external magnetic field parallel to the \bar{c} axis ($\vec{H} \parallel \bar{c}$). These lines collapsed into a single line for magnetic field orientation of $\theta \cong 54^\circ$ approximately with respect to the \bar{c} axis in the \bar{a} - \bar{c} plane. The angular dependence of these lines is attributed to crystalline-field effects; the effect of anisotropic susceptibility on our spectra can be ignored in the first approximation as have been supported also by independent magnetization measurements. The absence of some of the expected fine-structure lines as well as the anisotropic angular dependence of the linewidth of some of the transitions in our spectra could be explained by random internal stress model. We demonstrate that random strains exist also in other systems like LaSb:Gd. The thermal broadening of the $\frac{1}{2} \leftrightarrow -\frac{1}{2}$ transition in the $\vec{H} \parallel \bar{c}$ orientation is much larger than that of the collapsed line in qualitative (but not quantitative) agreement with the theory of Plefka and Barnes.⁶⁻⁸ Analysis of the g shift and the Korringa thermal broadening of LaNi₅:Gd yields a very large exchange enhancement factor provided that the Gd conduction-electron exchange coupling is not strongly \bar{q} dependent. This supports the idea that LaNi₅, similar to the Pd,¹⁵ is an "almost ferromagnetic" metal.

In annealed single crystals of LaNi₅:Gd, the ESR results exhibit a "ferromagnetic resonance" appropriate to the hexagonal symmetry. The origin of this resonance is not clearly understood at present but it

is most probably due to induced magnetism in the host by slight chemical changes (migration of Ni and La, or changes in the strain field) in the "almost ferromagnetic" compound.

II. EXPERIMENTAL RESULTS

The $\text{LaNi}_5\text{:Gd}$ intermetallic compounds were prepared by repeating melting in an arc furnace at argon atmosphere. We have used Gd and La of 99.9% purity and Ni of 99.999% purity from Leico Industries. Rods having cylindrical shape were, then, prepared from the molten LaNi_5 using a special arrangement in our arc furnace. These rods were used to grow single crystals by the electron-beam furnace technique. X-ray examination confirms single crystals of 6 mm diameter and elongation of 30 mm approximately. The single crystals were cut into smaller cylinders (to fit our cavity and Dewar), using an electroerosion machine, with the \bar{c} and an \bar{a} axis perpendicular to the cylinder axis. The single-crystal cylinders were, then, electroetched in a solution containing 20% water, 20% Glycerin, and 60% phosphoric acid by volume, using a current density of approximately 2 A/cm^2 . The nominal Gd concentrations were 0.25 at. %, 0.20 at. %, 0.05 at. %. Some of the samples were annealed in Argon atmosphere for a week at a temperature of 1100°C . X-ray examinations after annealing reveal hexagonal single crystals appropriate to the LaNi_5 phase.

The ESR measurement were carried out mostly at X band ($\nu = 8.9 \text{ GHz}$) in the temperature range between 1.8 and 15 K. The samples were rotated around the cylinder's axis so that the magnetic field lies in the \bar{a} - \bar{c} plane of the crystal. One sample of $\text{LaNi}_5\text{:Gd}$ (2000 ppm) was measured at Q band during a visit of one of us (D.S.) to the Free University of Berlin. In addition, magnetization measurements were performed using vibrating-type magnetometer. Our experimental results are significantly different for annealed and as cast (unannealed) single crystals and can be summarized, as follows:

A. Cast samples

(i) Measurements at X band on unannealed samples of $\text{LaNi}_5\text{:Gd}$ reveal several resolved anisotropic lines. Figure 1 exhibits some experimental spectra. As clearly seen, there are *three* resolved resonance lines which are observed for external field parallel to the \bar{c} axis [see also Fig. 1(a)]. These lines collapsed into a single line when the crystal was rotated towards $\theta = 54^\circ$ [Fig. 1(b)] (here θ is the angle between the \bar{c} axis and the magnetic field direction \bar{H} in the plane of rotation, the \bar{a} - \bar{c} plane). For magnetic field in the

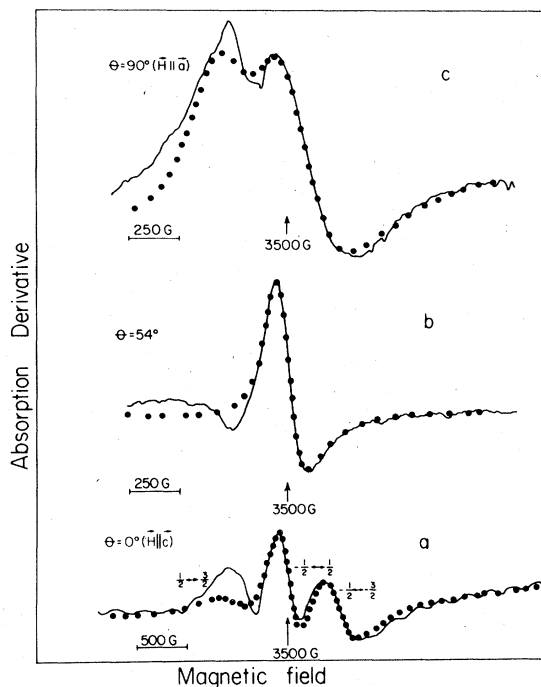


FIG. 1. ESR spectra of $\text{LaNi}_5\text{:Gd}$ (0.2%) at temperature of $T = 1.8 \text{ K}$ and for several magnetic field orientations. The solid lines represent the experimental spectra; the closed circles a theoretical fit using a sum of Lorentzian lines together with the appropriate oscillator strength and population factors. The deviation of theory from experiment at the low-field side of the experimental spectra is attributed to the presence of "background signal" as explained in the text. θ in Fig. 1 represents the angle between the magnetic field \bar{H} and the \bar{c} axis in the plane of rotation (the \bar{a} - \bar{c} plane). The measurements were carried at $\nu = 8.9 \text{ GHz}$.

\bar{a} direction, the spectrum exhibits two barely resolved lines [Fig. 1(c)]. The determination of the field for resonance and the linewidth of the individual resonance lines was carried out by fitting the observed spectra with a sum of Lorentzian line shapes (see Fig. 1). The fitting procedure is slightly complicated by the presence of a broad background signal mainly at low fields as well as by the presence of a $g \approx 2$ resonance. The background signal, originates with our samples, is probably due to possible non-stoichiometric Ni present in our samples. The presence of the background signal does not allow detailed analysis of the low-field lines in our spectra. It should be mentioned that the fields for resonance, as determined by fitting the experimental line shape to a sum of Lorentzian lines, are identical with those extracted using Barnes-Plefka analysis (but see Sec. III for details).

(ii) In Fig. 2, we have plotted the angular depen-

dence (at $T=1.8$ K) of the field for resonance of the individual lines in Fig. 1. The field for resonance was extracted by the fitting procedure described above. The angular dependence of the linewidth at 1.8 and 4.2 K of two of our lines (to be denoted hereafter as the $-\frac{1}{2} \leftrightarrow \frac{1}{2}$ transition and $-\frac{3}{2} \leftrightarrow -\frac{1}{2}$ transition, but see below for detailed analysis) is shown in Fig. 3. As seen, the linewidth of the $-\frac{1}{2} \leftrightarrow \frac{1}{2}$ transition exhibits anisotropic behavior with a minimum in the linewidth at about $\theta \cong 54^\circ$.

(iii) The temperature dependence of the field for resonance of the $-\frac{1}{2} \leftrightarrow \frac{1}{2}$ and the $-\frac{3}{2} \leftrightarrow -\frac{1}{2}$ transitions in the \bar{c} direction is shown in Fig. 4. As clearly seen, no significant temperature dependence is observed. We noted, however, that the intensity of the $-\frac{3}{2} \leftrightarrow -\frac{1}{2}$ line decreases faster than the intensity of

the $-\frac{1}{2} \leftrightarrow \frac{1}{2}$ transition.

(iv) The thermal broadening of the $-\frac{1}{2} \leftrightarrow \frac{1}{2}$ transition in the $\bar{H} \parallel \bar{c}$ direction was also measured and was found to be 9 ± 3 G/K. This thermal broadening is larger than the thermal broadening of the collapsed line ($\Theta \cong 54^\circ$) which is 3 ± 1.5 G/K. These thermal broadenings should be considered with caution as the "residual width" due to other mechanisms is relatively large. In the presence of large residual width a deconvolution technique is needed to estimate the exact thermal broadening.

(v) At Q band only a single line with anisotropy in the field for resonance was observed clearly; its linewidth is about 600 G. A background signal around 12 600 G has prevented detailed analysis of the transition.

(vi) Magnetization measurements of our single cry-

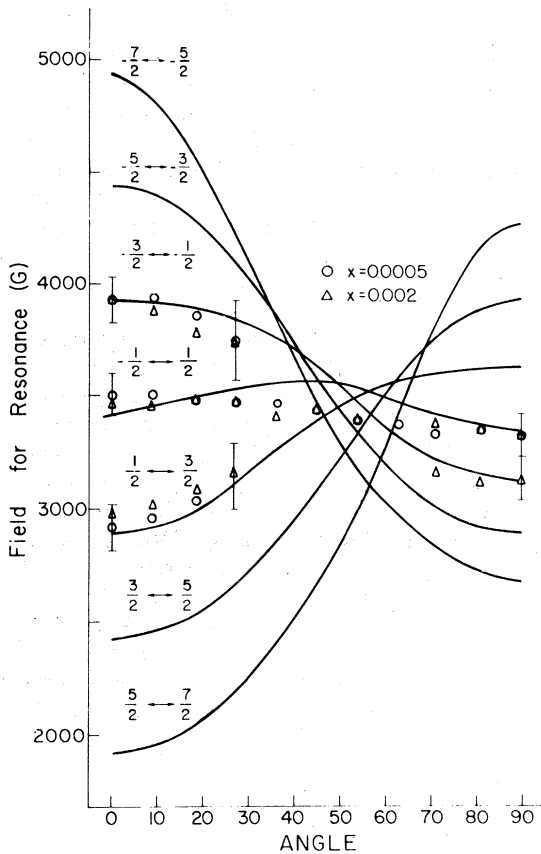


FIG. 2. Angular dependence of the field for resonance of the individual lines as determined by our fitting procedure (in Fig. 1). The circles and triangles represent results for two different samples, i.e., $x=0.0005$ (500 ppm) and $x=0.002$ (2000 ppm) in $Gd_xLa_{1-x}Ni_5$. The solid lines are theoretical fits with Eq. (1) using the following parameters: $D=250$ G and $g=1.85$.

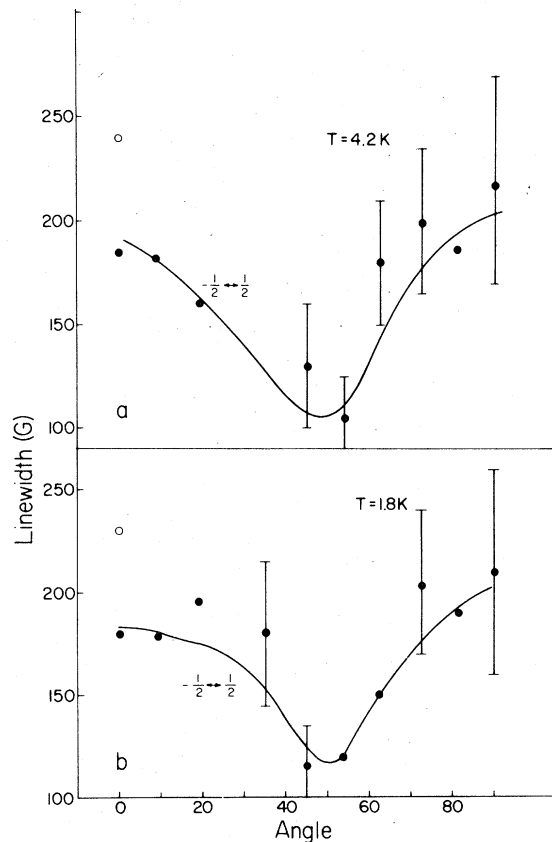


FIG. 3. Angular dependence of the linewidth of the $-\frac{1}{2} \leftrightarrow \frac{1}{2}$ transition (closed circles) at (a) $T=4.2$ K and (b) $T=1.8$ K. As seen the linewidth exhibits a minimum at $\theta \cong 54^\circ$ from the \bar{c} axis in the $\bar{a}-\bar{c}$ plane. For comparison the width of the $-\frac{1}{2} \leftrightarrow -\frac{3}{2}$ line for $\theta=0$ is also given (open circle).

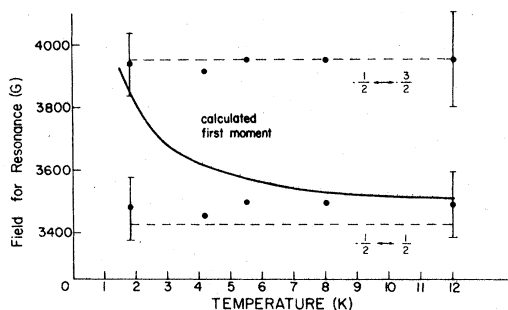


FIG. 4. Temperature dependence of the field for resonance (as determined by our fitting procedure in Fig. 1) for the $-\frac{1}{2} \rightarrow -\frac{3}{2}$ and $-\frac{1}{2} \rightarrow \frac{1}{2}$ lines. The dashed lines are the theoretical field for resonance expected for these lines respectively assuming $D = 250$ G and $g = 1.85$ (see text). The solid line represents the calculated "first moment" (see Ref. 1) using the parameters $D = 250$ G and $g = 1.85$.

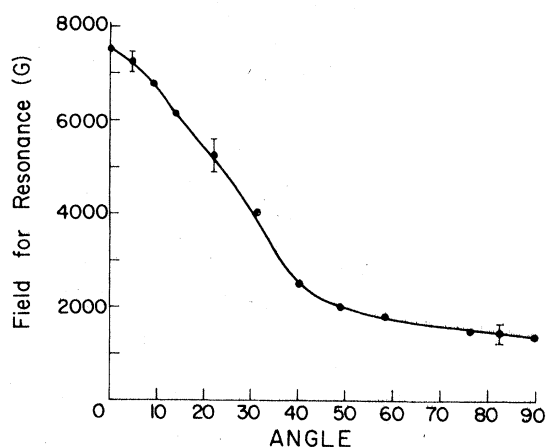


FIG. 6. Field for resonance of the "ferromagnetic line" observed in one of our annealed $\text{LaNi}_5\text{:Gd}$ single crystals. $T = 4.2$ K.

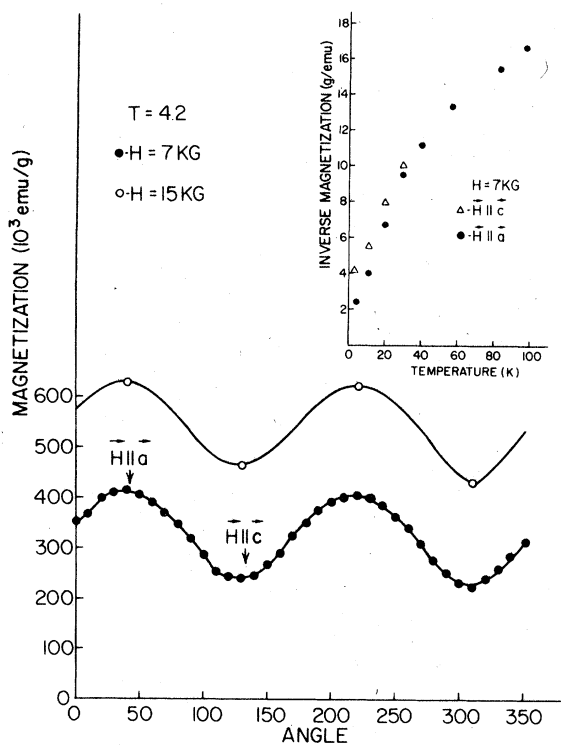


FIG. 5. Angular dependence of the magnetization of "pure" LaNi_5 single crystal at $T = 4.1$ K and for two different external fields. The magnetic field was rotated in the $\bar{a}\bar{c}$ plane. The inset represents the inverse magnetization for $\bar{H} \parallel \bar{c}$ and $\bar{H} \parallel \bar{a}$, respectively, in different temperatures. As clearly seen from the inset the difference of the inverse magnetization for these two orientations decreases with increasing temperature. This indicates that the observed angular anisotropy, at least partially, is due to the presence of magnetic impurities (but see text).

stals reveal significant anisotropy appropriate to hexagonal symmetry. The anisotropy decreased with the increase of temperature (Fig. 5). This feature supports the idea that the observed anisotropy is mostly associated with the presence of magnetic impurities or excess of Ni ions in our samples. Thus, it is not easy to extract the host anisotropic susceptibility.

B. Annealed samples

After annealing, an additional strong anisotropic line appeared. The line intensity and its angular dependence almost did not change up to room temperature. The linewidth and the position were different in different samples. The angular dependence of this line in a sample where it shows a relatively simple behavior is shown in Fig. 6. The field for resonance in the \bar{c} direction is about 7500 G and decreases to 1400 G when the crystal is rotated towards the \bar{a} direction. Its linewidth in the \bar{a} direction is about 200 G. The observed signal is characteristic of ferromagnetic resonance in hexagonal environment.¹⁶ Magnetization measurements of annealed samples show some hysteresis which was not observed for the rest of the samples studied.

III. ANALYSIS

In the present section we shall demonstrate that our experimental features for as cast $\text{LaNi}_5\text{:Gd}$ single crystals can be explained by axial field Hamiltonian for Gd^{3+} in the hexagonal symmetry as well as by a random strain model. The spin Hamiltonian of Gd^{3+} , in axial symmetry and in the presence of an external

magnetic field, is given by¹⁷

$$\mathcal{H}_c = \mu_B [g_{\parallel} S_z H_z + g_{\perp} (S_x H_x + S_y H_y)] + D [S_z^2 - (\frac{1}{3}) S(S+1)] \quad (1)$$

Here D is the axial crystalline-field parameter, H is the external magnetic field, μ_B is the Bohr magneton, and for generalization,¹⁷ we have assumed that the g value might be anisotropic with g_{\parallel} and g_{\perp} as the values of g for magnetic field in the \bar{c} and \bar{a} directions, respectively. Seven resonance lines associated with the $M \leftrightarrow M-1$ transitions are expected¹⁷; here M are the expectation values of S_z . In the notation of Abragam and Bleaney,¹⁷ we have identified the resonance lines in the \bar{c} direction as the $-\frac{3}{2} \leftrightarrow -\frac{1}{2}$, $-\frac{1}{2} \leftrightarrow \frac{1}{2}$, and $\frac{1}{2} \leftrightarrow \frac{3}{2}$ transitions [Fig. 1(a)]; the two lines in the \bar{a} direction are identified as the $-\frac{1}{2} \leftrightarrow \frac{1}{2}$ and $-\frac{3}{2} \leftrightarrow -\frac{1}{2}$ transitions [Fig. 1(c)]. The solid lines in Fig. 2 are the best fit of Eq. (1) to the observed angular dependence of the field for resonance. The fact that the intensity of the high-field line [the $-\frac{3}{2} \leftrightarrow -\frac{1}{2}$ line in Fig. 1(a)] decreases faster than the intensity of $-\frac{1}{2} \leftrightarrow \frac{1}{2}$ transition upon increasing tem-

perature indicates that the sign of D is positive. The fitting procedure yields the following parameters: $D = +250 \pm 30$ G, $g = g_{\parallel} = g_{\perp} = 1.85 \pm 0.01$. The g value observed is consistent with that observed in powdered samples.¹²⁻¹⁴

Clearly, the most disturbing feature in Fig. 1 and our theoretical fit in Fig. 2 is the absence of some of the transitions in our experimental spectra. While the absence of the $\frac{5}{2} \leftrightarrow \frac{7}{2}$ and $\frac{3}{2} \leftrightarrow \frac{5}{2}$ transitions could be partially understood by the small thermal population factor associated with these transitions, this is not the case of the lines $-\frac{5}{2} \leftrightarrow -\frac{7}{2}$ and $-\frac{3}{2} \leftrightarrow -\frac{5}{2}$ which are also absent. We propose an internal random stress model^{18,19} to explain both the absence of these transitions as well as the anisotropy of the linewidth shown in Fig. 3. We argue that such a model leads to a larger "residual width" for $M \leftrightarrow M-1$ transitions having larger M value. Details of our calculations and assumption are given in the Appendix. Here we just quote the second moment $\langle(\delta H)^2\rangle_{M,M-1}$ associated with random strain distribution for the various $M \leftrightarrow M-1$ transitions. We found for the $M \leftrightarrow M-1$ transition in the $\bar{a}\bar{c}$ plane, the following second moment:

$$\langle(\delta H)^2\rangle_{M,M-1} = \langle[HA_1 + (2M-1)B_1]^2\rangle (3 \cos^2\theta - 1)^2 + \langle[HA_2 + (2M-1)B_2]^2\rangle \sin^2\theta \quad (2)$$

where the factors A_1 , A_2 , B_1 , and B_2 are given in the Appendix in terms of the average of the deformation components ϵ_{pq} ; H is the external magnetic field. Equation (2) can explain (at least qualitatively) some of our experimental features. First, as clearly seen from Eq. (2), our second-moment calculation predicts a minimum linewidth at $\theta = 54^\circ$ ($3 \cos^2\theta - 1 = 0$) provided that the second term in Eq. (2) can be neglected with respect to the first term. A minimum of the linewidth at $\theta = 54^\circ$ is consistent with our experimental observation for the $-\frac{1}{2} \leftrightarrow \frac{1}{2}$ transition in Fig. 3. The dominance of the first term in Eq. (2) requires that the deformation component $\langle\epsilon_{pp}\rangle$ is much larger than the deformation component $\langle\epsilon_{pq}\rangle$ $p \neq q$ which is a reasonable assumption. Second, it is seen that the second moment $\langle(\delta H)^2\rangle_{M,M-1}$ increases with M . The dependence of $\langle(\delta H)^2\rangle_{M,M-1}$ on M should be most pronounced under the condition $|B_1| > HA_1$. This last condition, is probably satisfied at X band as the width of the $\pm\frac{1}{2} \leftrightarrow \pm\frac{3}{2}$ transitions is significantly larger than the width of the $-\frac{1}{2} \leftrightarrow \frac{1}{2}$ transition (Fig. 3). The larger width of the $\pm\frac{1}{2} \leftrightarrow \pm\frac{3}{2}$ line with respect to the $-\frac{1}{2} \leftrightarrow \frac{1}{2}$ line provides additional evidence for the existence of random strains in our samples.

A more quantitative analysis, Eq. (2), predicts that the random strain contribution to the linewidth of the $-\frac{1}{2} \leftrightarrow \frac{1}{2}$ transition vanishes for $\theta = 54^\circ$ provided that the second term in Eq. (2) can be neglected. Thus, we shall take the minimum linewidth of the $-\frac{1}{2} \leftrightarrow \frac{1}{2}$ transition at $\theta \cong 54^\circ$ as the "background width" due to contributions other than the random strain. Experimentally this width is ~ 120 G (Fig. 3). For a Gaussian distribution of stresses, then, the individual linewidth associated with the $M \leftrightarrow M-1$ transition at low temperatures can be expressed

$$\Delta H_{M,M-1} = 1.17 [(120)^2 + \langle(\delta H)^2\rangle_{M,M-1}]^{1/2} \quad (3)$$

The linewidth $\Delta H_{M,M-1}$ is angular dependent and can be calculated provided that the value of B_1 is known [see Eq. (2)]. The value of B_1 can be estimated (under our assumptions above) from the experimental linewidth of the $-\frac{1}{2} \leftrightarrow \frac{1}{2}$ or the $-\frac{3}{2} \leftrightarrow -\frac{1}{2}$ transitions using Eq. (3). To demonstrate the dependence of $\Delta H_{M,M-1}$ on M , we have calculated the width of the various transitions for the $\bar{H} \parallel \bar{c}$ direction. We find

$$\Delta H_{-1/2, 1/2} \approx 150 \text{ G}, \quad \Delta H_{\pm 1/2, \pm 3/2} \approx 250 \text{ G} \quad (4)$$

$$\Delta H_{\pm 3/2, \pm 5/2} \approx 350 \text{ G}, \quad \Delta H_{\pm 5/2, \pm 7/2} \approx 450 \text{ G} \quad (5)$$

It should be mentioned that the distribution of stresses is not necessarily a Gaussian and looks more like a Lorentzian but a Gaussian was assumed for simplification. We have used the values of $\Delta H_{M,M-1}$ in Eqs. (4) and (5) to calculate the ESR line shape for magnetic field in the \bar{c} direction. The line-shape calculation was carried out using the transverse dynamic susceptibility given by Urban *et al.*²⁰ This dynamic susceptibility was derived using the Barnes-Plefka theory for the nonbottleneck regime and is given by

$$\chi^+(\omega) \sim 1 - \omega [\sum_{M,M'} P_M(\Omega^{-1})_{M,M'}] , \quad (6)$$

where M and M' are quantum numbers describing the various S_z states, P_M are transition probabilities, defined by Urban *et al.*,²⁰ for transitions from the M to $M-1$ states, and the matrix elements $\Omega_{M,M'}$ are given by

$$\Omega_{M,M'} = \left(\frac{\hbar\omega}{g\mu_B} - H - H_{M,M-1} \right) \delta_{M,M'} - i\Delta H_{M,M-1} \delta_{M,M'} - \left[\frac{i}{2} \right] \Delta H_K C_{M'} (2\delta_{M,M'} - \delta_{M,M'+1} - \delta_{M,M'-1}) , \quad (7)$$

where $\omega/2\pi$ is the microwave frequency, $H_{M,M-1}$ is the field for resonance of the $M \leftrightarrow M-1$ transition given in Fig. 2, $\Delta H_{M,M-1}$ is the "residual width" which contains the random strains contribution and is given by Eqs. (4) and (5), ΔH_K is the Korringa relaxation rate, and $C_{M'}$ is a matrix element given by $C_{M'} = S(S+1) - M'(M'+1)$.

The theoretical spectra for a magnetic field parallel to the \bar{c} axis is given in Fig. 7(b). The agreement with the experimental spectra, given in Fig. 7(a) after subtracting the background signal, is good. Although not shown here, the agreement between experiment and theory is good also for other magnetic field orientations.

Although it will not be discussed in detail, the observation of a single line at Q -band frequency (presumably the $-\frac{3}{2} \leftrightarrow -\frac{1}{2}$) and the absence of other transitions can be explained by the thermal population factors as well as by the presence of random strains. It should be stressed, however, that in this case one should take into consideration higher-order terms proportional to $H_p S_q^3$ and $H_p^2 S_q^2$ in the stress Hamiltonian (See Appendix).

We turn now to analyzing the thermal broadening. The thermal broadening observed for the collapsed position (of 3 ± 1.5 G/K) is determined by the Korringa mechanism according to the theory of Barnes-Plefka.⁶⁻⁸ This thermal broadening is given, in the absence of \bar{q} dependence of the exchange interaction, as

$$\frac{\Delta H_k}{T} = \frac{\pi k_B}{g\mu_B} (\Delta g_0)^2 F_d K(\alpha) , \quad (8)$$

where Δg_0 is the g shift induced by the exchange coupling with the conduction electrons ($\Delta g_0 = -0.15 \pm 0.01$ in our experiment), k_B is the Boltzmann factor, F_d is a constant associated with the degeneracy of the d states at the Fermi level (usually $F_d \sim 1/5$, see Ref. 21), $K(\alpha)$ is the "Moriya" function associated with the electron-electron Coulomb in-

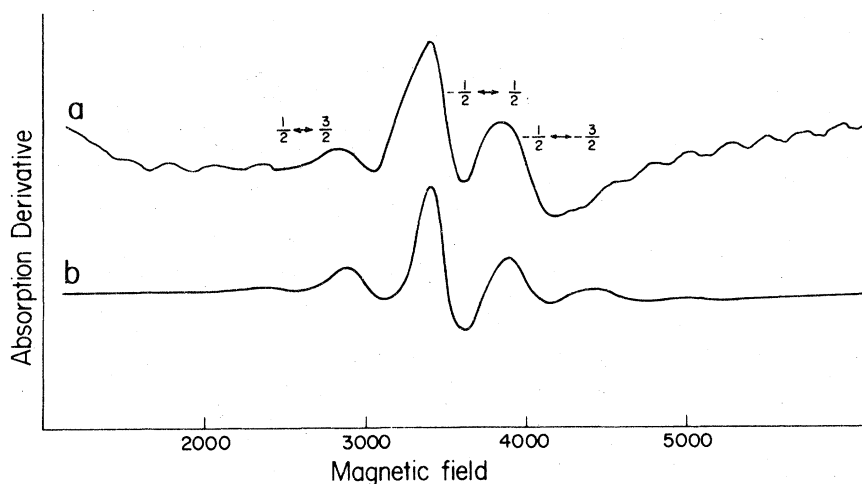


FIG. 7. (a) Experimental ESR spectra of LaNi₅:Gd (2000 ppm) for $\bar{H} \parallel \bar{c}$ and after subtracting the "background" signal. $T = 1.8$ K. (b) Theoretical spectra for $\bar{H} \parallel \bar{c}$ using the Barnes-Plefka theory [Eqs. (6) and (7)] together with the various experimental parameters mentioned in the text. $T = 1.8$ K.

interaction U , leading to exchange enhancement of the host susceptibility, and α is the enhancement factor.^{21,22} Using Eq. (8), as well as our results, we have estimated $K(\alpha)$ to be $K(\alpha) \approx 2 \times 10^{-2}$. This yields an enhancement factor of $\alpha \sim 0.86$, for spatially constant U and $\alpha \sim 0.98$ for δ function range of U .²¹ These values of α should be considered with caution because we have not considered possible wave-vector dependence of the exchange interaction²³ as well as possible multiband contributions.²⁴ However, these effects cannot explain a factor of 10^{-2} difference between the experimental thermal broadening and the one calculated from the g shift using Eq. (8). Thus, our experimental results strongly support a large enhancement factor in LaNi_5 . This might indicate that LaNi_5 is an "almost itinerant ferromagnet" of the Stoner type.

The thermal broadening of the $-\frac{1}{2} \leftrightarrow \frac{1}{2}$ transition in the \bar{c} direction, of 9 ± 3 G/K, is much larger than that in the collapsed position in qualitative agreement (but not quantitative!) with the theory of Barnes-Plefka.²⁰ According to this theory, one can expect an enhancement of 16 for the thermal broadening of this transition with respect to the Korringa mechanism. Experimentally, we have observed, however, an enhancement between two and eight due to the large experimental error in the determination of the thermal broadening.

Finally, it is interesting to note that the thermal broadening of the $\frac{1}{2} \leftrightarrow -\frac{1}{2}$ transition in the $\bar{H} \parallel \bar{c}$ orientation is comparable to that found for the thermal broadening of Gd in powdered samples of LaNi_5 .^{12,14} This might indicate that the spectra in powdered LaNi_5 :Gd originates with the $\frac{1}{2} \leftrightarrow -\frac{1}{2}$ transition.

IV. DISCUSSION

We shall discuss, first, the observation of the additional line in annealed samples of LaNi_5 (Fig. 6). The large intensity of this line (even at room temperature), the almost temperature independence of its angular position and the similarity of its angular dependence to that observed in ferromagnetic samples,¹⁶ indicate that this line is a ferromagnetic resonance. The angular dependence appropriate to hexagonal symmetry supports the idea that the ferromagnetic domains are single crystals with \bar{c} axis parallel to that of the LaNi_5 single-crystal axis. The possibility that this resonance arises from domains of hexagonal Ni is rejected because hexagonal Ni is not ferromagnetic.²⁵ It is possible that slight chemical changes produced by the annealing process (i.e., migration of La or Ni) induce ferromagnetism in the "almost ferromagnetic" LaNi_5 compound. If this is the case, however, then the relatively large ferromagnetic tran-

sition temperature which is above room temperature is not understood. Evidence that annealing effects might be important in LaNi_5 is provided by Siegmann *et al.*²⁶ These authors have demonstrated that during annealing, La ions diffuse to the surface and consequently there is a deficiency of La or excess of Ni at certain depth in LaNi_5 single crystal. Another possibility for the interpretation of ferromagnetic resonance is the formation of macroscopic regions of $\text{La}_2\text{Ni}_{17}$ in the LaNi_5 by the annealing process. The structure of $\text{La}_2\text{Ni}_{17}$ is very close to that of LaNi_5 and can be obtained from the latter by replacing one La ion by two Ni ions in the base of the LaNi_5 hexagonal unit cell. $\text{La}_2\text{Ni}_{17}$ is probably ferromagnetic as the analogue compound Y_2Ni_{17} is ferromagnetic below $T_c \approx 150$ °K.²⁷ Thus, although no change in the lattice constant was observed after annealing, there is the possibility of formation of a macroscopic region of another phase (like $\text{La}_2\text{Ni}_{17}$) after annealing which gives rise to the observed ferromagnetic resonance. Clearly, a systematic study of the nature of the magnetism in annealed single crystals of LaNi_5 is required. Whatever the origin of the ferromagnetic resonance, the possibility to induce magnetism by slight chemical changes (annealing) is an exciting prospect and should be carefully studied.

Another very interesting feature of our results is the observation of large internal random strain contributions in LaNi_5 :Gd. Random strains have been reported previously in LaSb:Dy ,¹⁹ and Ag:Dy ,²⁸ and although unnoticed, probably exist also in many other systems. For instance, the ESR spectra of Gd in the cubic LaSb crystal²⁹ have shown that the width of the $-\frac{7}{2} \leftrightarrow -\frac{5}{2}$ transition is much broader than the $-\frac{1}{2} \leftrightarrow \frac{1}{2}$ transition in the [001] direction; also the $-\frac{7}{2} \leftrightarrow -\frac{5}{2}$ transition is broader in the [001] direction with respect to the same transition in the [111] direction. These features support the existence of random strains in LaSb:Dy . Figure 8(b) exhibits a theoretical line shape, calculated using Eq. (6) together with random strains for the case of LaSb:Dy in the [001] direction. As clearly seen, the theoretical spectra is very similar to the experimental LaSb:Dy spectra [Fig. 8(a)]. For comparison the theoretical spectra in the absence of random strains is given in Fig. 8(c). This indicates that random strains play an important role in the ESR of rare-earth ions in very dilute alloys, much more than was anticipated before. In the case of LaNi_5 , Buschow and Van-Mal¹⁰ have demonstrated that LaNi_5 has large homogeneous regions where La ions substitute for Ni ions in a random fashion and vice versa. This is accompanied by slight changes in the unit-cell dimensions. Certainly this can provide a possible origin for the random internal strains. In conclusion:

(a) We have observed resolved ESR spectra for Gd in LaNi_5 single crystals (as cast samples) for the first

time. The observation of resolved fine structure in LaNi₅:Gd is associated, according to the theory of Plefka-Barnes,⁶⁻⁸ with the very small Korringa width with respect to the crystal electric-field parameter, D (i.e., $D/\Delta H_K \approx 25$). This is in contrast to the rest of the hexagonal hosts¹⁻³ where $D/\Delta H_K$ is approximately 1 in the temperature range in consideration.

(b) We have shown that the ESR spectra of Gd in LaNi₅ is strongly influenced by internal random strains. Especially the absence of some of the observed transitions for LaNi₅:Gd spectra is due to random strains and not to exchange narrowing effects. To demonstrate that exchange narrowing effects are

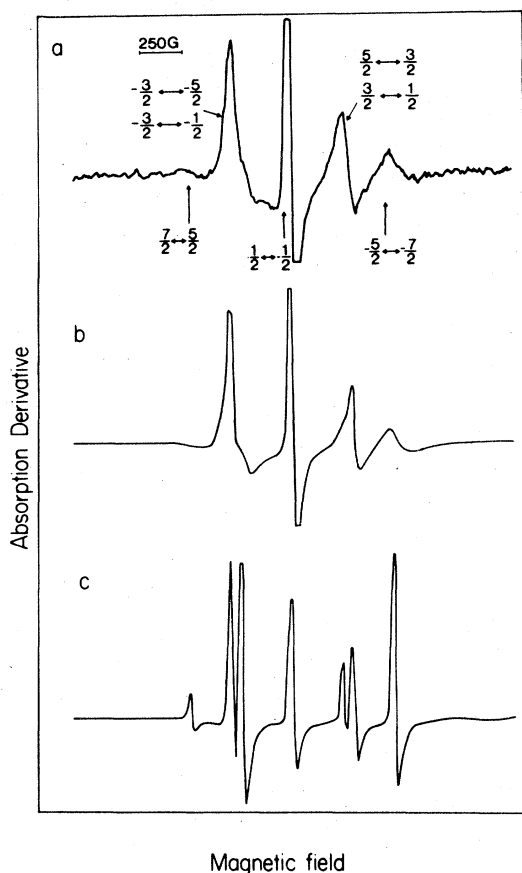


FIG. 8. (a) Experimental spectra of LaSb:Gd (500 ppm) at X-band frequency, $T = 1.4$ K in the [100] direction. This spectra was taken from Ref. 29. (b) Calculated spectra, using Eqs. (6) and (7), for Gd in cubic symmetry in the [100] direction and assuming the presence of random strains. The spectra was calculated using the following parameters: $g = 1.99$, $b_4 = 30$ G, $A_1 = 3.3 \times 10^{-3}$ G, $B_1 = 8.2$ G, $A_2 = B_2 = 0$. (c) The same as in (b) but neglecting random strains, i.e., $g = 1.99$, $b_4 = 30$ G, $\Delta H_{M, M-1} = 20$ G (independent of M).

not important in the present case, we have calculated the "first moment"¹⁻³ which takes into account both the angular dependence of the individual $M \leftrightarrow M - 1$ transitions as well as the thermal population factors. Such "first moments" have been shown in the past to fit very well the temperature and angular dependence of the field for resonance of the Gd³⁺ single ESR line in exchanged narrowed systems.¹⁻³ Figure 4 exhibits our first-moment calculation using $D = 250$ G. As seen, its temperature dependence is significantly different from the *temperature-independent* field for resonance of the experimental lines (Fig. 4). This further supports the idea that the exchange narrowing mechanism is not important in LaNi₅:Gd.

(c) The thermal broadening of the $-\frac{1}{2} \leftrightarrow \frac{1}{2}$ transition is very similar to that previously observed in powdered samples of LaNi₅:Gd.¹²⁻¹⁴ This might indicate that the powdered spectra originates with the $-\frac{1}{2} \leftrightarrow \frac{1}{2}$ transition. This is also supported by the equality between the residual width of the line observed in very dilute powders^{12,13} and that of the $-\frac{1}{2} \leftrightarrow \frac{1}{2}$ transition. Consequently ESR of powders of LaNi₅:Gd should be reanalyzed.

(d) Our results indicate very small anisotropy in the g value of Gd in LaNi₅. We estimate the anisotropic g shift to be less than 15% of the total g shift ($\Delta g \sim -0.15$). The measured anisotropic susceptibility (Fig. 5) is not inconsistent with this observation.

(e) We have shown that LaNi₅ exhibits large host exchange enhancement and is "almost ferromagnetic" of Stoner type. Evidence for ferromagnetic domains in annealed single crystals might be associated with this property.

Note added in proof: After submission of the paper we found out that L. Schlapbach from Zurich (to be published) has measured the susceptibility of LaNi_{4.96}. His susceptibility at 100 K is 5×10^{-6} emu/g, smaller than the susceptibility value observed by Buschow for LaNi₅ of $\chi \approx 14 \times 10^{-6}$ emu/g and our value of 9×10^{-6} emu/g at 100 K. This indicates that, indeed, it is the excess of Ni which contributes to the larger susceptibility in our measurements.

ACKNOWLEDGMENTS

We would like to thank Mr. J. M. Bloch for the permission to use the temperature control system which was built by him, and Professor K. Baberschke for stimulating discussions and for his permission to use the unpublished results of the ESR of Gd in LaNi₅ at the Q band. We would also like to thank Mr. A. Gabai for developing the proper electro-etching solution. This research was supported by a grant from the U.S.-Israel Binational Science Foundation (B.S.F.), Jerusalem.

APPENDIX

The spin Hamiltonian of Gd^{3+} ion in axial crystalline field and in the presence of stresses may be written

$$\mathcal{H} = \mathcal{H}_c + \mathcal{H}_1 + \mathcal{H}_2, \quad (A1)$$

where \mathcal{H}_c is the Hamiltonian (1), \mathcal{H}_1 and \mathcal{H}_2 are terms that describe the influence of the stresses. \mathcal{H}_1 is given by

$$\begin{aligned} \mathcal{H}_1 = & [g_1(\Gamma_1)E^{(1)}(\Gamma_1) + g_2(\Gamma_1)E^{(2)}(\Gamma_1)](2H_zS_z - H_xS_x - H_yS_y) + g(\Gamma_5)[E_1(\Gamma_5)\{S_x, H_z\} + E_2(\Gamma_5)\{S_y, H_z\}] \\ & + g(\Gamma_6)[E_1(\Gamma_6)(S_xH_x - S_yH_y) + E_2(\Gamma_6)\{S_x, H_y\}] \end{aligned} \quad (A2)$$

Γ_i are the irreducible representations of the hexagonal group. The strains are given by

$$\begin{aligned} E^{(1)}(\Gamma_1) &= \epsilon_{xx} + \epsilon_{yy} + \epsilon_{zz}, \\ E^{(2)}(\Gamma_1) &= 2\epsilon_{zz} - \epsilon_{xx} - \epsilon_{yy}, \\ E_1(\Gamma_5) &= \epsilon_{xz}, \quad E_2(\Gamma_5) = \epsilon_{yz}, \\ E_1(\Gamma_6) &= \epsilon_{xx} - \epsilon_{yy}, \quad E_2(\Gamma_6) = 2\epsilon_{xy} \end{aligned}$$

and

$$\{H_p, S_q\} = H_p S_q + H_q S_p, \quad p, q = x, y, z.$$

Due to the axial symmetry we have also

$$\langle \epsilon_{xx} \rangle = \langle \epsilon_{yy} \rangle, \quad \langle \epsilon_{xz} \rangle = \langle \epsilon_{yz} \rangle,$$

where the brackets $\langle \rangle$ indicate the averaging over the random strains ϵ_{pq} . The term \mathcal{H}_2 is bilinear in \bar{S} and is written the same way as \mathcal{H}_1 , but H_p is replaced by S_p and $g_j(\Gamma_\alpha)$ by other constants $G_j(\Gamma_\alpha)$ in Eq. (A2).

Assuming that the crystalline-electric-field (CEF) part of the Hamiltonian is a small perturbation on the Ziman part, we can use the eigenfunctions, $|M\rangle$, of

the Ziman Hamiltonian in order to calculate the energy shifts that result from the strains. From Eqs. (A1) and (A2) we obtained the shift of the resonance field of $M \leftrightarrow M-1$ transition in the $\bar{a}\text{-}\bar{c}$ plane to be

$$\begin{aligned} & [HA_1 + (2M-1)B_1](3\cos^2\theta - 1) \\ & + [HA_2 + (2M-1)B_2]\sin 2\theta, \end{aligned} \quad (A3)$$

where

$$A_1 = g_1(\Gamma_1)E^{(1)}(\Gamma_1) + g_2(\Gamma_1)E^{(2)}(\Gamma_1), \quad (A4)$$

$$A_2 = g(\Gamma_5)E_1(\Gamma_5). \quad (A5)$$

B_i can be obtained from Eqs. (A4) and (A5) by changing the interaction constants $g(\Gamma_\alpha)$ by $G(\Gamma_\alpha)$. θ is the angle between the external magnetic field and the c axis. The randomness of the strains permit us to write the strain contribution to the residual width of the $M \leftrightarrow M-1$ transition, assuming statistical independence of the $E^{(j)}(\Gamma_1)$ and $E_i(\Gamma_5)$, as

$$\begin{aligned} \langle \delta H^2 \rangle_{M, M-1} &= \langle [HA_1 + (2M-1)B_1]^2 (3\cos^2\theta - 1)^2 \\ &+ [HA_2 + (2M-1)B_2]^2 \sin^2\theta \rangle. \end{aligned}$$

¹L. J. Tao, D. Davidov, R. Orbach, D. Shaltiel, and C. R. Burr, Phys. Rev. Lett. **26**, 1438 (1971).

²B. Elschner and G. Weimann, Solid State Commun. **9**, 1935 (1971).

³J. Nagel and K. Baberschke, in *Crystal Field Effects in Metals and Alloys*, edited by A. Furrer (Plenum, New York, 1977).

⁴M. B. Salamon, Phys. Rev. Lett. **26**, 704 (1971).

⁵P. H. Zimmermann, D. Davidov, R. Orbach, L. J. Tao, and J. Zitkova, Phys. Rev. B **6**, 2783 (1972).

⁶T. Plefka, Phys. Status Solidi B **51**, K113 (1972).

⁷T. Plefka, Phys. Status Solidi **55**, 129 (1973).

⁸S. E. Barnes, Phys. Rev. B **9**, 4789 (1974).

⁹S. Nasu, H. H. Neumann, N. Marzouk, R. S. Craig, and W. E. Wallace, J. Phys. Chem. Solids **32**, 2779 (1971).

¹⁰K. H. J. Buschow and H. H. Van Mal, J. Less-Common Met. **29**, 203 (1972).

¹¹J. H. N. Van Vucht, F. A. Kuijpers, and H. C. A. M. Bruming, Philips Res. Rep. **25**, 133 (1970); F. A.

Kuijpers, Philips Res. Rep. Suppl. **2**, (1973); H. H. Van Mal, K. H. J. Buschow, and A. R. Miedema, J. Less-Common Met. **35**, 65 (1974).

¹²D. Davidov, Ph.D. thesis (Hebrew University, Jerusalem, 1970) (unpublished).

¹³D. Davidov and D. Shaltiel, Phys. Rev. Lett. **21**, 1975 (1968).

¹⁴S. E. Male and R. H. Taylor, J. Phys. F **5**, L26 (1975).

¹⁵J. M. Moret, R. Orbach, M. Peter, D. Shaltiel, J. T. Suss, W. Zingg, R. A. B. Devine, and P. H. Zimmermann, Phys. Rev. B **11**, 2002 (1975).

¹⁶H. S. Jarrett and R. K. Waring, Phys. Rev. **111**, 1223 (1958).

¹⁷A. Abragam and B. Bleaney, *Electron Paramagnetic Resonance of Transition Ions* (Oxford University, London, 1970).

¹⁸A. M. Stoneham, Rev. Mod. Phys. **41**, 82 (1969).

¹⁹D. Davidov, V. Zevin, J. M. Bloch, and C. Rettori, Solid

- State Commun. 17, 1279 (1975).
- ²⁰P. Urban, D. Davidov, B. Elschner, T. Plefka, and G. Sperlich, Phys. Rev. B 12, 72 (1975).
- ²¹A. Narath, in *Hyperfine Interaction*, edited by A. J. Freeman and R. B. Frankel (Academic, New York, 1967); A. Narath and H. T. Weaver, Phys. Rev. 175, 373 (1968).
- ²²T. Moria, J. Phys. Soc. Jpn. 18, 516 (1963).
- ²³D. Davidov, K. Maki, R. Orbach, C. Rettori, and E. P. Chock, Solid State Commun. 12, 621 (1973); D. Davidov, C. Rettori, R. Orbach, A. Dixon, and E. P. Chock, Phys. Rev. B 11, 3546 (1975).
- ²⁴G. Barberies *et al.*, Phys. Rev. B 19, 2385 (1979).
- ²⁵H. Remy, *Treatise on Inorganic Chemistry* (Elsevier, Amsterdam, 1956), Part II, p. 309.
- ²⁶H. C. Siegmann, L. Schlapbach, and C. R. Brundle, Phys. Rev. Lett. 40, 972 (1978).
- ²⁷J. Laforest, R. Lemair, D. Paccard, and R. Pauthenent, C. R. Acad. Sci. Ser. B 264, 676 (1967).
- ²⁸S. B. Oseroff and R. Calvo, Phys. Rev. B 18, 3041 (1978).
- ²⁹C. Rettori, D. Davidov, A. Grayevsky, and W. M. Walsh, Phys. Rev. B 11, 4450 (1975).